

Satellite Altimeter Detection of Global Very Extreme Sea States (VESS)

V. J. Cardone¹, A. T. Cox¹, M. A. Morrone¹,
and Val R. Swail²

¹Oceanweather Inc
Cos Cob, CT, USA

²Environment Canada
Downsview, Ontario, Canada

1. INTRODUCTION

When forced by high quality wind fields, third-generation spectral ocean wave models perform very well over most of the dynamic range of naturally occurring wave regimes. However, there has been reported (e.g. Cardone et al, 1996) a tendency for reduced skill and some negative bias in specification of very extreme sea states (VESS), which we refer to here as significant wave height (HS) greater than 14 meters, a range that in many open sea regions encompass design level (i.e. recurrence intervals of 10-years or greater) conditions. Therefore, it can be expected that further improvements in physics or numerics of wave models will be aided by model tests that include tropical and extra tropical storms that may generate VESS. Specification of atmospheric forcing in such storms of sufficient accuracy that wind field errors do not mask model physics effects has been difficult in the past due to the typical sparseness of open-ocean in-situ marine wind measurements, but within the past two decades great advances in monitoring the time and space evolution of surface wind fields of hurricanes by airborne flight level and surface wind sensors (e.g. Powell et al. 2009), and of extratropical storms by satellite mounted passive and active microwave marine surface wind sensors (e.g. Cardone et al., 2004) have made accurate wind field specifications possible and an example is given in this paper.

Wave model physics testing is, of course, only one source of interest in VESS. The UN IOC JCOMM Expert Team on Wind Waves and Storm Surges has noted the need for high quality measured wave data sets in the open ocean for use in model validation, forecast verification, satellite calibration and marine climatology and has supported the development of a JCOMM-label data base of wave measurements in extreme storm seas (Soares and Swail, 2006). In addition, the vessel and platform design and vessel sea-keeping communities are very interested in the incidences of extreme individual wave crests (Buchner and Bunnik (2007) and wave heights (Gannett and Gemmrich, 2009) that occur within the context of VESS.

2. IN-SITU MEASUREMENTS OF VESS

In this study we are not so much interested in the absolute frequency of occurrence of VESS but in the detection of storms associated with VESS and the peak storm detected VESS, so in general we select only one peak VESS per storm. VESS have become increasingly sampled in recent years by ship borne wave recorders (SBWR) and buoy and platform wave measurement systems, particularly as buoy and platform systems have been deployed further offshore, especially in the eastern North Atlantic Ocean (NAO) and Gulf of Mexico (GOM). VESS sampled by SBWRs include the peak HS of about 18.5 m measured by *RRS Discovery* in the intense eastern North Atlantic “Rockall Trough” storm event (Holliday et al., 2006) and a peak HS of 15.5 m in November, 2001 by the SBWR on *Polarfront* at Ocean Station Mike (Magnusson et al., 2006).

Measurements by moored buoys in winter storms include the peak HS of 16.9 m and 14.6 m measured by Canadian MEDS buoys 44137 and 44141 respectively in the “Halloween Storm” of October, 1991 (Cardone et al., 1996), a peak HS of 16.9 m at US NDBC Nomad hull buoy 46003 in the northeast North Pacific Ocean (NPO) in January, 1991 and a peak HS of 14.2 m on December 3, 2007 at NDBC 3m discus buoy, which is moored about 100 km west of the Portland, Oregon. The K-buoy array in the eastern NAO have recorded VESS in several recent events most notably a peak HS of about 18.3 m at K-3 (also WMO number 62108) on December 8, 2007. Notable buoy measurements in the northern GOM in recent hurricanes include a peak HS of in Hurricane Ivan (September, 2004) of 16.0 m at NDBC 3 m discus buoy 42040 (Cox et al., 2005) a peak HS of 16.9 m at the same buoy in Hurricane Katrina in August 2005 (Cardone et al., 2007). In these cases, the locations of the measurements with respect to the storm and the often many lower estimates from surrounding sites, suggest that these VESS are at or close to the maxima in the associated storm.

Offshore platform mounted sensors are mainly downward looking radars and lasers and WAMOS and MIROS scanning radars. Magnusson et al. (2006) evaluated such measurements from several platforms in the Norwegian Sea in the severe storm of January, 2006 and assess that the storm peak HS was about 15.5 m in the Haltenbanken region offshore central Norway. Platforms measurements of VESS in the northern GOM in the recent hurricanes include 14.2 m at *Redhawks* in Hurricane Rita of September, 2005 and 15.4 m at *Marlin* in Hurricane Ivan (2004) (Forristall, 2007).

As noted above, taken together, the in-situ measurement locations sample a very small portion of the global oceans with a distinct bias toward the margins of the major basins. Also, all cited cases are from the Northern Hemisphere. Therefore, to sample the whole globe more or less uniformly so as to greatly increase the population of VESS events and possibly to extend the sample to even greater wave heights than sampled to date in-situ, a global scan of available altimeter wave heights was undertaken.

3. ALTIMETER DATASETS

The altimeter datasets applied in this study are from the TOPEX/POSEDON, JASON-1 and ENVISAT satellites. The TOPEX/POSEDON was launched August 10, 1992 and data from the TOPEX instrument was processed for the period of September 1992 to September 2004. All TOPEX data were obtained from the Physical Oceanography Distributed Active Archive Center (PODAAC) Generation-B (MGDR-B) dataset. To account for drift in the TOPEX significant wave height estimates over time, a time-based correction was applied to the data as described in Queffeuilou (2004). JASON-1 was launched in December, 2001. Its data were also obtained from PODAAC and a correction applied based on buoy inter-comparisons (Picot et al. 2003). Data from the JASON-1 instrument were applied over the period of January 2002 to December 2007. While JASON-1 provides significant wave height estimates from both its Ku and C band instruments, only the Ku band data were considered here. ENVISAT RA2 was launched in March, 2002. Its data were obtained from the European Space Agency (ESA) and covers the period of September 2002 to December 2007. Quality control measures and buoy corrections were applied as described in Queffeuilou (2003). Therefore, no fast-delivery (FD) altimeter data streams were used for this study as such data should be expected to possess different and probably greater errors than the final delivery products (e.g. Durrant et al., 2009).

The satellite-specific correction factors have been typically derived from inter-comparison of altimeter estimates with collocated buoy significant wave height measurements. Table 1 gives the linear regressions applied and sources. In this study, we are interested in a range of HS that is clearly outside the calibration range of typical buoy-altimeter collocated data sets. At an HS of 14 m, the JASON-1 and ENVISAT adjustments are both only + 14 cm. There is the potential that the scatter and bias in the altimeter HS

estimates are greater in the VESS range including a possible dependence on wave steepness (Janssen, 1997), though an exploration of this dependence by Durrant et al. (2009) using fast delivery products suggests that this effect can account for bias of the order +/- 10 cm. Still, since there is the potential for greater bias and uncertainty in the HS range of interest here, the threshold of VESS detection was lowered to 12 m in the initial scan so as to ensure that we capture all VESS above the 14 m threshold of interest.

Table 1 Altimeter data sets

Satellite	Period Scanned	Calibration Applied	Source
TOPEX	Sept, 1992 – Sept, 2004	Time Variable	Queffeuilou 2004
JASON-1	Jan, 2002 – Dec. 2007	$HsAdj=1.0072*Hs+0.092$	Picot et al. 2003
ENVISAT	Sept. 2002 – Dec 2007	$HsAdj=1.0327*Hs-0.183$	Queffeuilou 2003

3. VESS DETECTION

The basic plan of the study was to scan all altimeter datasets noted above, as corrected and at the highest intrinsic sampling rate, typically 1 Hz, to identify all “real” occurrences of detected storm peak HS in storms that exceed HS of 12m, summarize the spatial distribution and range of those occurrences and extract associated meteorological characteristics of the parent storms from global reanalysis data products and remotely sensed surface marine wind data.

Despite the best efforts of the agencies responsible for processing the altimeter wave products to produce a clean, quality controlled archive of altimeter data free of errors, there remain a considerable number of spurious “spikes” in the processed data, which makes a purely objective and fully automated identification of the storm peak VESS virtually impossible. Such spikes tend to originate during transition of the radar beam from land to ocean, near ice edges and in intense beam-scale convective storms. To lessen the effects of spikes, and as a first step in the process, the individual altimeter samples in the data streams from each separate instrument were first binned onto a ½ degree global grid and a median filter was applied. All local along-orbit maxima of HS found in this binned result provides a list of candidate storms that produced a peak HS above a threshold of 12 meters. This list was found to contain over 900 candidate peaks. Even a cursory scan of this candidate list, looking only at the contingent altimeter data stream (e.g. VESS occurring with a very low sampled altimeter wind speed combined with very large differences between the Ku-band and C-band estimates (for JASON-1 and ENVISAT) of HS and the along-orbit time scale of the build-up and decay indicated that the majority of the 900 + candidates were spurious spikes.

Since median filtering did not remove all spurious spikes in the raw altimeter data, additional quality control and filtering was accomplished by cross-referencing each of the 900+ candidates against coincident meteorological data. This was done by first producing for each candidate a plot of the raw altimeter data (wind speed and HS) within a +/- 90-minute time window of the apparent altimeter peak on a background of the co-incident NCEP/NCAR reanalysis (NRA) surface pressure fields interpolated to 3-hourly intervals. Figure 1 is an example of such a plot, in this case corresponding to the highest occurrence found in the final surviving population of events, namely a VESS of 20.24 m sampled by JASON-1 in the central NAO near 2100 UTC on February 9, 2007. The apparent VESS peaks are shown along the color-coded orbit segments as large red dots. This same plot also shows an obvious isolated spurious spike of HS of about 20 m in the Gulf of Papua that had already been rejected by the median filter. Each such plot was scanned by a meteorologist to identify real VESS cases associated with coincident or precedent severe storms as opposed to spurious spikes. This scan filtered the vast majority of spurious spikes though a few additional cases were found only after examining more detailed time

sequences of surface pressure analyses together with all conventional ship and buoy observations and satellite sensed marine winds from QuikSCAT for 6-hourly sequences from 48-hours before the time of each VESS to 12-hours following.

The automated and meteorologist-aided quality control and filtering produced a final file of storm peak VESS consisting of 260 members. The distribution of these cases by satellite and basin is given in Table 2 for thresholds of 12 m and 14 m and 16 m. The global distribution is shown in Figure 2 for each threshold. In summary, there are found 36 cases in the NAO, 54 cases in the NPO and 170 cases in the Southern Oceans (SO). Overall the number of cases is proportional to the size of the basin, but especially after considering the relative basin sizes there is a tendency for a density of storms and the most intense storms (with regard to VESS) to occur in the smallest basin (the NAO) which is a bit surprising. The table shows that within the NPO and SO about 38% of the cases detected have peak HS > 14 m and about 7% > than 16 m, while in the NAO those percentages are 44% and 14% respectively. For example, if one just compares the NAO and the South Atlantic Ocean, whose areas between the 30th and 60th parallels are approximately equal the relative NAO/SAO occurrences of HS> 12 m, > 14 m, >16 m are 36/26, 16/9 and 5/1 respectively (not shown in Table 2) SAO). Of course, the total VESS counts and attributions to basin and class are relative, not absolute, because there are no doubt events that are missed. In fact, it appears that virtually all VESS that occurred within tropical cyclones were missed as we could identify only one event in each hemisphere that might be associated with tropical cyclones and both of those were in the vicinity of 30 degrees (N or S) latitude. We make no attempt to estimate the detection rate.

Table 2 Distribution of Detected VESS Storm Peaks

Satellite	North Atlantic	North Pacific	Southern Oceans	Total
TOPEX Hs >12	7	9	16	32
> 14	2	5	3	10
> 16	2	1	1	4
JASON Hs >12	27	40	138	205
> 14	14	15	58	87
> 16	3	3	10	16
ENVISAT > 12	2	5	16	23
> 14	0	1	3	4
> 16	0	0	0	0
TOTAL Hs > 12	36	54	170	260
> 14	16 (44%)	21 (39%)	63 (38%)	100 (38%)
> 16	5 (14%)	4 (7%)	10 (6%)	19 (7%)

Table 3 VESS events equal to or above 14 meters detailed by satellite and basin

Southern Oceans					North Pacific					North Atlantic				
CYMDH	Lat.	Long.	Satellite	Hs Peak (m)	CYMDH	Lat.	Long.	Satellite	Hs Peak (m)	CYMDH	Lat.	Long.	Satellite	Hs Peak (m)
2006100903	-53.431	110.430	JASON	18.9	2006021318	45.004	189.618	JASON	17.5	2007020922	48.287	340.794	JASON	20.2
2005081918	-45.728	64.732	JASON	18.6	2006020213	43.066	160.227	JASON	17.2	2003030812	46.580	318.568	JASON	17.2
2002073107	-58.399	68.192	TOPEX	18.1	2005122306	40.208	162.291	JASON	16.3	2003021209	48.117	319.358	TOPEX	16.8
2007091218	-49.098	39.607	JASON	17.5	2003022201	35.491	169.673	TOPEX	16.2	2007010115	45.909	316.365	JASON	16.7
2003040711	-55.533	56.380	JASON	16.6	2004010906	35.710	192.226	TOPEX	15.9	2002012122	42.230	328.009	TOPEX	16.6
2004062318	-57.140	22.970	JASON	16.6	2007031211	32.873	183.970	JASON	15.7	2007022120	47.683	323.155	JASON	15.1
2006061302	-50.581	236.316	JASON	16.4	2002112319	38.958	177.348	JASON	15.2	2006032416	38.060	318.097	JASON	15.0
2002120415	-51.586	19.642	JASON	16.3	2006011815	39.049	171.382	JASON	15.1	2004030208	56.950	335.897	JASON	14.8
2005051521	-43.626	76.018	JASON	16.3	2002120317	39.159	177.208	JASON	15.0	2002012415	45.191	320.778	JASON	14.7
2004091603	-57.474	250.502	JASON	16.2	2005111315	41.788	161.101	JASON	15.0	2006021208	53.519	330.240	JASON	14.6
2003090215	-48.070	149.233	JASON	15.9	2003120813	48.288	172.290	JASON	14.8	2006012306	51.219	310.136	JASON	14.4
2004053108	-54.659	151.965	JASON	15.7	2003022700	37.628	182.490	TOPEX	14.7	2003011421	53.537	335.885	JASON	14.3
2002051620	-40.040	68.620	TOPEX	15.7	2005102116	47.099	210.341	JASON	14.7	2005011310	49.493	319.447	JASON	14.3
2006060510	-58.285	36.757	JASON	15.7	2003121503	47.817	195.743	JASON	14.5	2002123017	41.953	320.911	JASON	14.2
2006072420	-51.767	82.641	JASON	15.7	2002010603	33.781	170.719	TOPEX	14.4	2002011517	51.377	318.827	JASON	14.0
2006052710	-56.104	52.324	JASON	15.7	2002110719	40.988	226.914	JASON	14.4	2002020712	54.779	326.487	JASON	14.0
2005090213	-47.810	89.432	JASON	15.6	2002121207	42.907	170.014	TOPEX	14.4					
2007040314	-52.800	230.625	JASON	15.6	2005021520	41.523	186.834	JASON	14.2					
2005110509	-53.920	78.783	JASON	15.5	2005090502	29.812	131.465	ENVISAT	14.2					
2003041322	-49.216	119.286	JASON	15.4	2005100921	49.866	167.722	JASON	14.2					
2006041423	-52.095	346.684	JASON	15.4	2003010410	31.367	193.307	JASON	14.0					
2004080912	-60.996	242.031	JASON	15.2										
2007091310	-54.229	37.905	JASON	15.1										
2007082123	-52.694	23.858	JASON	15.0										
2007083009	-51.505	96.476	JASON	15.0										
2004070905	-59.284	165.057	JASON	15.0										
2006081818	-48.332	36.116	JASON	15.0										
2004092014	-56.112	72.186	JASON	14.9										
2006091202	-50.551	194.514	JASON	14.8										
2003040803	-54.286	63.510	JASON	14.7										
2005062110	-53.549	17.051	JASON	14.7										
2007081810	-58.632	125.400	JASON	14.6										
2002081302	-43.450	79.753	JASON	14.6										
2007013110	-52.128	9.413	JASON	14.6										
2004062511	-54.094	123.886	JASON	14.5										
2007041819	-53.793	0.399	JASON	14.5										
2007043012	-54.053	68.820	JASON	14.5										
2003060110	-58.235	169.872	JASON	14.4										
2006071119	-52.664	137.693	JASON	14.4										
2002073014	-54.977	54.456	TOPEX	14.4										
2004110622	-61.476	255.402	JASON	14.4										
2006101122	-54.554	171.642	JASON	14.4										
2006092011	-41.745	33.036	JASON	14.4										

2005042213	-58.734	168.143	JASON	14.4
2007042221	-60.277	54.811	JASON	14.3
2007082911	-52.789	78.332	JASON	14.3
2007080508	-61.691	283.053	JASON	14.3
2002090323	-52.707	72.549	JASON	14.3
2006070209	-46.172	79.428	JASON	14.2
2003041406	-44.621	123.351	JASON	14.2
2006062317	-48.795	90.294	ENVISAT	14.2
2005042808	-39.816	336.906	JASON	14.2
2006032010	-59.950	270.288	JASON	14.1
2005040904	-53.861	326.477	JASON	14.1
2006082000	-52.027	53.090	JASON	14.1
2004091516	-51.558	51.190	JASON	14.1
2006102103	-54.248	66.285	JASON	14.1
2007051020	-41.328	40.988	JASON	14.0
2006041622	-57.235	95.802	JASON	14.0
2002103112	-53.638	62.532	JASON	14.0
2003042615	-52.240	181.054	TOPEX	14.0
2002090802	-43.362	124.418	JASON	14.0
2005052614	-52.916	142.606	JASON	14.0

Table 3 gives a master list of all cases of VESS equal to or above 14 m. Table 4 gives a summary of the minimum central pressure and deepening rate of the associated cyclone averaged over cases in each basin. For the cases that occurred during the QuikSCAT period, kinematic properties of each storm such as maximum surface wind speed and duration of wind speeds above 50 knots of the “fetch-zone” or “jet streak” apparently responsible for the peak VESS and the propagation speed of the streak may be gleaned from available QuikSCAT data and such analysis is underway. For example, in the storm of February 7, 2007, associated with a bona-fide peak of about 20 m (not accounting, of course, for unknown biases, if any, in the altimeter data at this upper reach of the dynamic range) the associated extratropical cyclone formed south of Nova Scotia on February 8 and moved northeastward across the NAO attaining its maximum intensity (minimum central pressure) of 952 mb near 50 N, 30 W at 0600 February 9, which is about 15 hours prior to the JASON-1 pass that sampled the peak VESS. Over the 24-hour period proceeding the time of minimum pressure, the central pressure fell from 988 mb to 952 mb, or a deepening rate of 36 mb/24 hours, well above the “bombogenesis” or explosive cyclogenesis threshold described first by Sanders and Gyakum (1980). The average forward speed of the cyclone was close to 25 knots. This storm was very well monitored by QuikSCAT, which measured an “adjusted” (as described in more detail below) peak wind speed of 83 knots, and an apparent duration of peak wind speeds above 50 knots of at least 36-hours. This event was subjected to a detailed wind field reanalysis and wave hindcast as described in the next section along with the QuikSCAT wind speed adjustment method.

4. HINDCAST OF FEBRUARY 2007 NORTH ATLANTIC EVENT

Adjustment of Scatterometer Winds for Bias. On February 9th 2007 at 21:31 GMT the JASON-1 Ku-band altimeter measured an adjusted significant wave height of 20.2 meters (the C-band altimeter also measured an HS of 20.0 m) in the North Atlantic near 48.3N 19.2W. This was the highest significant wave height observed in the data set screened in this study, so this event was selected as the first to hindcast with an established 3G wave model. The reanalysis of the wind field involved the application of Oceanweather’s standard IOKA method implemented on a graphical user interface called the Wind

WorkStation (WWS) (Cox et al., 1995). Since the storm was so well monitored by QuikSCAT, which provides data at asynoptic times, a high temporal and spatial resolution manual kinematic analysis of the core of the event was undertaken, which depended, therefore, critically on a correct interpretation of the QuikSCAT winds.

Table 4 Storm peaks > 14m detected with mean minimum central pressure and maximum deepening rate

	North Atlantic	North Pacific	Southern Ocean
Number of Peaks	16	21	64
Minimum Pressure (mb)	960	964	951
Maximum Deepening Rate mb/24hrs	26	19	15

The storm in question was highlighted in the Mariners Weather Log review of North Atlantic Storms as the first storm monitored by QuikSCAT in which (it was claimed) wind speeds equivalent to Category 3 hurricane strength (Bancroft, 2007) were measured. A second storm following on the heels of the first storm is also described in which QuikSCAT peak wind speeds of about 95 knots were also measured but over a much smaller area than in the first storm. Reference is made in Bancroft (2007) to the use of “special parallel processing of 25-km” QuikSCAT data, which we believe refers to the application of the so-called QSCAT-1/F13 model function used to derive ocean wind vectors from backscatter measurements at NASA/JPL/Pasadena, CA (QuikSCAT Science Data Product User’s Manual). This model function replaced the QSCAT-1 model function developed during the mission validation/calibration phase and used for the standard so-called Level 2B processing of mission data between May 2, 2000 and the time of the switch to QSCAT-1/F13 in June, 2006. The entire mission data set has since been reprocessed using the revised model function so QSCAT-1 data are not available in Level 2B format post June, 2006. The QSCAT-1 and QSCAT-1/F13 yield essentially identical wind speeds up to about 16 m/s while the QSCAT-1/F13 wind speeds are greater than the QSCAT-1 winds above 16 m/s and increasingly so at higher and higher wind speeds. Differences in the retrieval of wind direction between the two algorithms appear to be slight.

Level 2B QSCAT-1 winds have been evaluated thoroughly at Oceanweather against all sources of ground truth including a sample of high quality winds measured by platforms in the North Sea. Level 2B QSCAT-1 winds have been integrated into the hindcast process for nearly a decade now and applied to many basins to produce unbiased specifications of the normal and extreme wave climates when used to force a proven 3G wave model, as summarized by Cardone et al. (2004). This evidence suggests that the new model function is introducing bias in retrieved wind speeds beginning at about 16 m/s, which becomes very significant at wind speeds important for diagnosis of wind fields in the types of storms responsible for VESS. This suspicion tends to be confirmed by a repeat of the statistical comparison of QuikSCAT winds speeds against the quality North Sea platform dataset but using the QSCAT-1/F13 data as opposed to the base algorithm. This is possible only for pre-June, 2006 data (again, JPL have not applied the QSCAT-1 model function to post-June, 2006 data) and the result for a three-year dataset (2000, 2001, 2005) is shown in Figure 3, where the similar analysis is shown for the base model function (but for a larger sample). The quantile-quantile wind speed plot for the F/13 dataset compares wind speed probability distributions computed from 33,133 collocated QuikSCAT-platform wind speed data-pairs. Up to the 90th percentile non-exceedance probability (about 18 m/s) the two algorithms are very similar but between the 99th percentile and 99.9th percentile the bias in the F/13 model function becomes increasingly evident. Statistical analysis of sensed winds by either the platform or QuikSCAT above 25 m/s indicate a mean positive bias in the F/13 wind speed of 3.09 m/s in a sample of 73 data-pairs in which

the platform wind speeds range up to 32 m/s. To minimize incorporation of this suspected bias in F/13 wind speeds into the kinematic analysis of the storm, the F/13 wind speeds were adjusted using a linear regression through a quantile-quantile scatter plot formed from 1-degree binned North Atlantic collocated base and F/13 QuikSCAT wind speeds as shown in Figure 4. The regression selected is the one fitted to F/13 wind speeds above 15 m/s. According to this regression an F/13 wind speed of 30 m/s is adjusted to 27.2 m/s. An F/13 wind speed of 49 m/s, corresponding to 95 knots, the peak F/13 wind speed sensed by the QuikSCAT scatterometer in the storm of February 7, is adjusted to 83 knots. Of course, this simple linear regression can not account for relative differences between QSCAT-1 and QSCAT-1/F13 as a function of incidence angle and beam polarization, but at least the major source of bias in the F/13 wind speeds has been addressed and minimized.

Kinematic Wind Field Reanalysis. The overall hindcast period allowed adequate time for spin-up and spin-down. For the bulk of this period the wind fields were derived by objective assimilation of all in-situ and QuikSCAT data into the NRA background analysis with the aid of a quality scan by a meteorologist to ensure no spurious measured data contaminated the fields and to aid the continuity of major kinematic centers of action. For the critical period of the evolution of the VESS storm of interest here, a series of 6-hourly kinematic analyses were drawn by the first author to maps that displayed all conventional measurements, NRA surface pressure analyses and adjusted 28-km QuikSCAT wind vectors, repositioned (up to 3-hours) within 300 nm of the storm center to conserve storm centered at analysis synoptic time from time of the pass, using the track of the storm pressure center. Given the pass times over the NAO, the 0600 UTC and 1800 UTC maps are typically rich in QuikSCAT coverage and the 0000 UTC and 1200 UTC maps relatively devoid of such data but a manual analysis can be very effective in propagating information from the data rich to data poor analysis times. An important first step in the kinematic reanalysis is to establish temporal continuity of the main kinematic features, especially the track and peak wind speed of the main surface wind speed jet streak that typically propagates eastward on the south side of the parent low with about its speed. The important of such jet streaks to strong wave response has been discussed by Cardone et al., (1996) and others.

Figure 5 shows a derived continuity map of the track of the parent low, its central pressure, the track of the main jet streak and the maximum wind therein between 1200 UTC February 8 and 0000 UTC February 10. As noted above, the evolution of central pressure indicates a minimum of 952 was attained at 0600 UTC February 9 while the NOAA Marine Ocean Prediction Center placed the minimum pressure at 949 mb 6 hours later, an honest difference considering the central pressure was not actually sampled. At the beginning of this detailed analysis period the maximum wind speed is already about 55 knots centered in a jet streak located about 120 nm south-southwest of the pressure center. Over the ensuing 12-hours, the maximum wind speed has increased to 75 knots and the radius of maximum wind has contracted to about 90 nm. The peak wind speed is analyzed as adjusted at 83 knots, at which time the radius of maximum wind has expanded to about 150 nm. The expansion continues over the following 24-hours as the peak winds slowly abate. At the time of the JASON-1 sampling of the peak VESS in this event, the peak wind speed is 62 knots and the radius of maximum wind is nearly 250 nm. The excellent coverage of QuikSCAT of this storm allows a specification of the temporal and spatial evolution of the main wave generation wind field kinematic properties and the specification of the absolute magnitude of the peak synoptic scale surface marine effective neutral wind speed of unprecedented accuracy for a storm of this class of extreme intensity. A peak average wind speed of 83 knots exceeds anything encountered by this analyst by a wide margin over a 40-year period of experience of kinematically reanalyzing hundreds of severe mid-latitude winter storms! Figure 6 shows a sequence of the hand analyses over the main part of the storm as digitized for assimilation and blending into the total wind field. The envelope of the final hindcast wind speed during the evolution of the storm is shown in Figure 7. The inner contour shown bounds an area of surface winds of greater than 42 m/s associated with west-

southwesterly wind directions that covered an area of sea surface of 29,000 square nm forcing the wave response found.

Wave Hindcast. The wave hindcast was executed on the same grid system and using the same wave model physics used for the MSC50 hindcast (Swail et al, 2006), namely a grid of average 30 nm spacing running Oceanweather's standard 3G physics (Khandekar et al, 1994; Forristall and Greenwood, 1998). The envelope of the peak HS response is shown in Figure 7. Note the area of 20 m HS that develops on the eastern edge of the area where wind speeds peaked, but this wave response is maintained eastward aided by propagation effects of course, even as the peak modeled wind speed decreases gradually. This plot suggests strongly that the peak HS response was essentially captured by the JASON-1 pass even though at first glance it might be surmised that the peak storm VESS were somewhat to the west and a bit earlier in the storm evolution. The maximum overall peak hindcast HS in this event was a bit higher at 21.09 m.

Figure 8 gives a snapshot of the HS field at the time of the JASON-1 pass and the lower panel compares directly the sampled 1Hz HS estimates and the hindcast HS interpolated to the position of the altimeter cells. Agreement is excellent at the storm peak with just a slight tendency for the hindcast pattern to run a bit high relative to the altimeter on the part of the transect that samples areas north and south of the maximum HS where spatial gradients in the wave field are high.

SUMMARY AND CONCLUSIONS

Interest in very extreme sea states (VESS; HS > 14 m) has been stimulated recently by the increasing number of measurements of VESS made in very intense tropical and extratropical storms in various NH basins by in-situ moored buoy and offshore platforms. VESS are of great interest to designers of vessels and offshore and coastal infrastructure and users of high-seas operational wave forecasts. The UN IOC JCOMM has recently called for the establishment of a community database of VESS occurrences. There is also the possibility that such sea states regimes will help to test new source term physics as they are incorporated into numerical spectral wave prediction models.

In this study, many millions of global satellite altimeter estimates from three missions (TOPEX, JASON-1, ENVISAT) spanning the period September, 1992 to December, 2007 were scanned, quality controlled, filtered and distilled using automated and man-machine mix procedures to identify 260 storms with storm peak HS > 12 m. The highest HS found was 20.2 m in the severe North Atlantic Ocean mid-latitude storm of February 9, 2007. Since this event was also well monitored by QuikSCAT, detailed and accurate wind forcing was developed for this event and used to drive a proven 3G wave model.

The principle conclusions of this study are:

The number of VESS storms detected is in general proportional to the size of the basins but normalized by the size of the basins it appears that the NAO spawns more VESS (extratropical) storms per unit area than any other basin. The NAO VESS storms also appear to generate the highest percentage of very extreme (HS > 16m) VESS storms.

All but a few of the cases detected were identified to be associated with extratropical cyclones. This reflects mainly the poor sampling of sea states in the inner core of tropical cyclones by satellite mounted nadir pointing altimeters.

QuikSCAT allowed high resolution and accurate specification of atmospheric forcing for the highest ranked VESS storm but the most recently adopted model function recommended by the NASA Wind Vector Science team (QSCAT-1/F13) is believed to be seriously biased high at wind speeds of interest to

VESS storms. Winds processed by or approximately adjusted back to the base model function QSCAT-1 are recommended for analysis of wind fields for VESS storms.

Peak wind speeds (equivalent neutral wind speed at 10-m elevation) in this storm were about 83 knots (adjusted) based on the analysis of QuikSCAT data and 95 knots according to the current /F13 scatterometer model function. Even the lower adjusted peak of 83 knots appears without precedent for an open ocean extratropical storm. This peak wind speed transforms, using a prevalent gust model to a peak sustained 1-minute wind speed (the reference interval used to rank hurricanes) of about 100 knots or 115 MPH, which correspond to a hurricane of Saffir-Simpson Category 3, though the scale of the wind field and the radius of maximum wind speed of this storm are much greater than typical of a hurricane. The term “Hurricane Force Extratropical Cyclones” (HFEC) to describe mid-latitude winter storms with hurricane wind speeds (Von Ahn et al., 2006).

With no iteration of the atmospheric forcing developed or the 3G wave model applied whatsoever, the hindcast was found to be in very close agreement with the JASON-1 HS transect of the highest ranked storm. This result provides tentative evidence that a proven “WAM-class” 3G model may be extended into the forcing range of severe “HFEC” with confidence as long as the forcing is accurately prescribed. To further explore this conclusion, we will next proceed to a hindcast as many of these VESS storms within the QuikSCAT mission period as feasible.

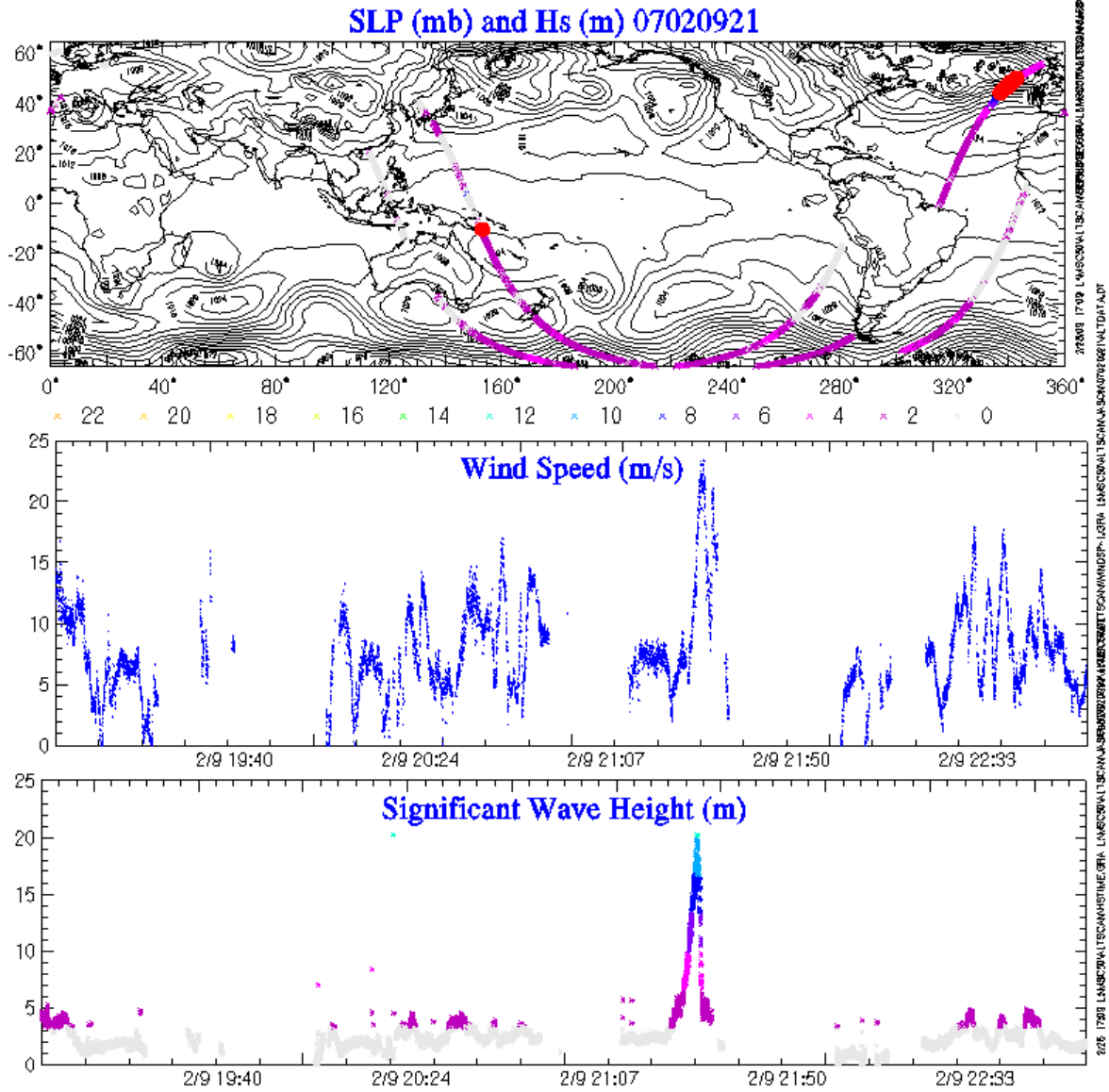


Figure 1. North Atlantic 20.24 meter event as measured by the JASON altimeter. Data shown +/- 90 minutes from Feb-09-2007 21 UTC.

Distribution of 12+ Meter Significant Wave Height
As Measured from the TOPEX, ENVISAT and JASON Altimeters

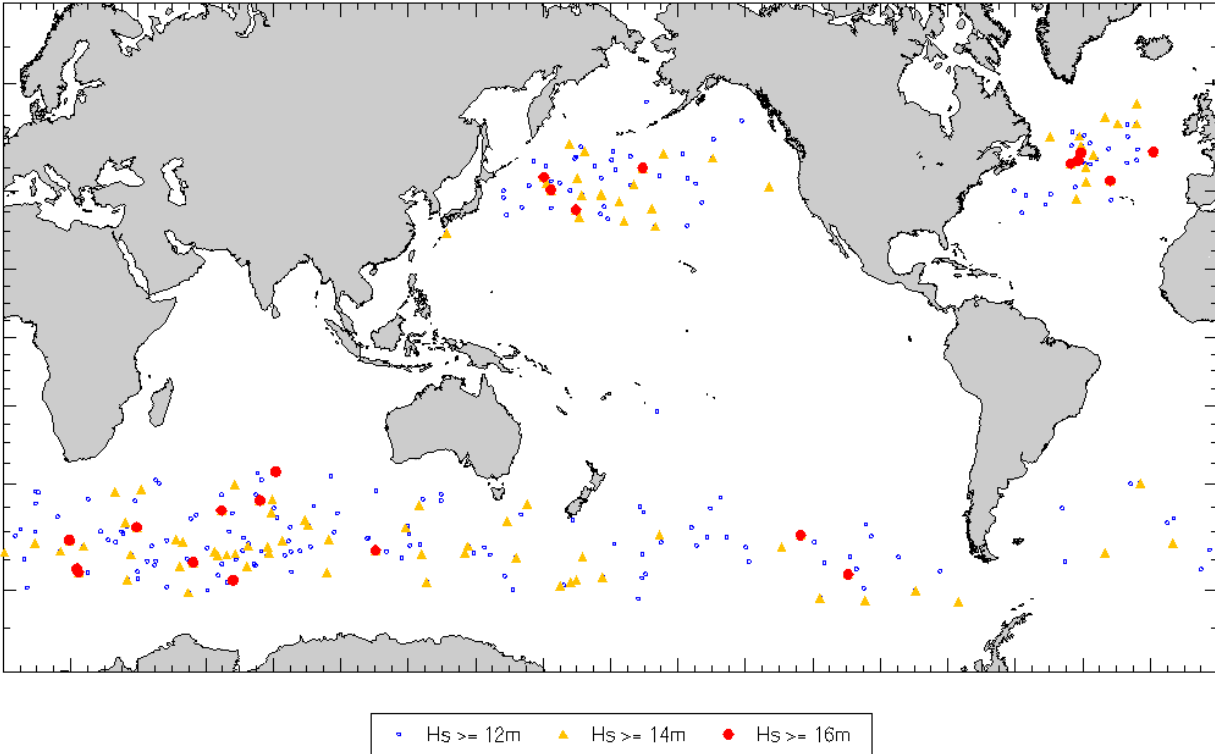


Figure 2. Global distribution of VESS events.

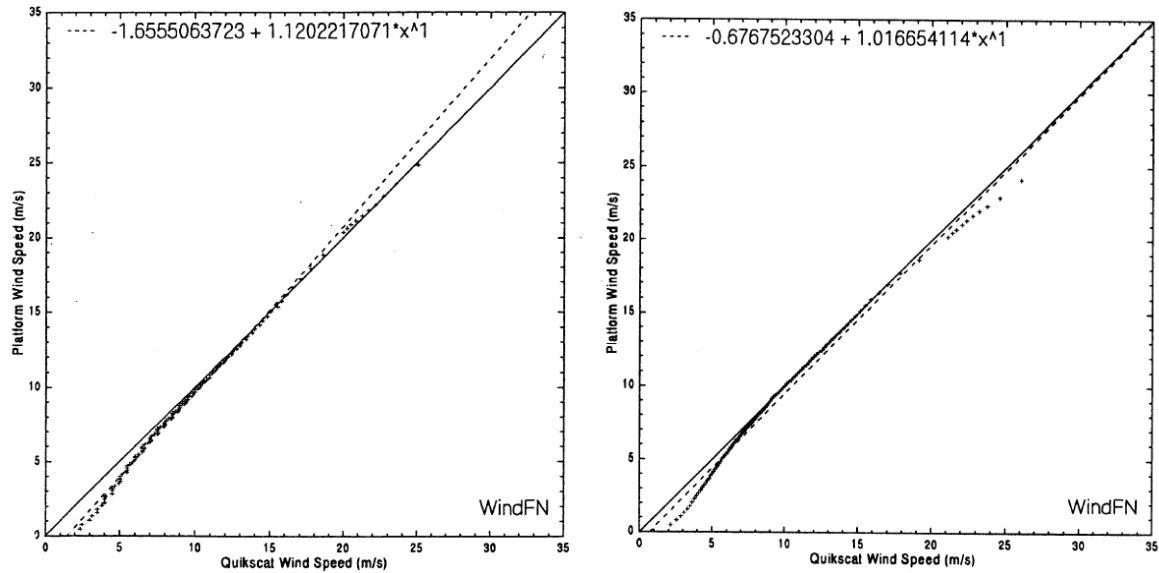


Figure 3. Quantile-Quantile (1-99.9%) of wind speeds from North Sea Platforms and QUIKSCAT scatterometer (QSCAT-1 left, QSCAT-1/F-13 right)

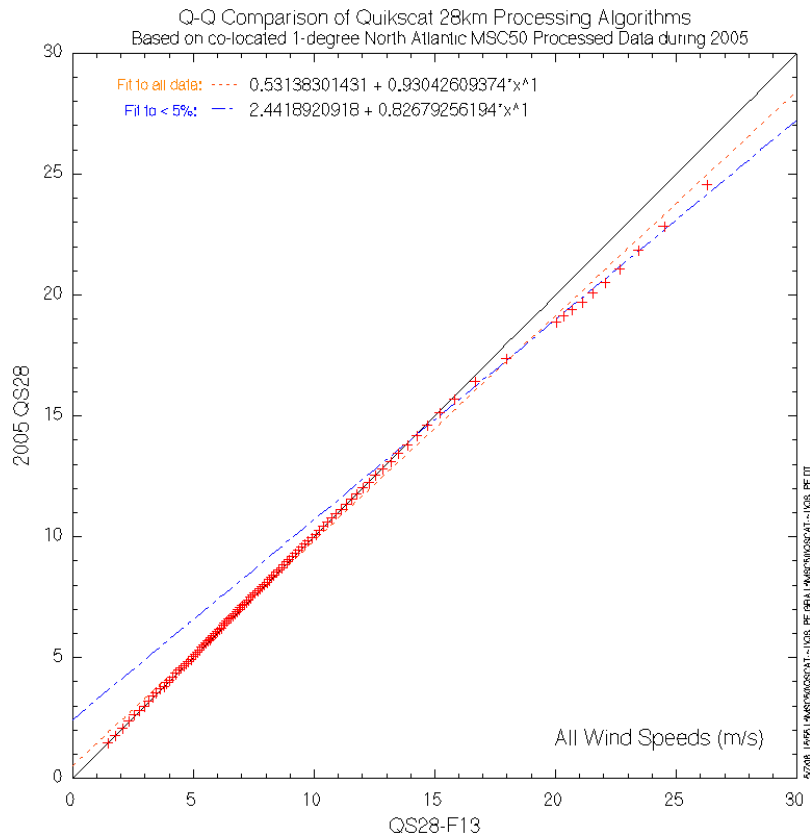


Figure 4. Quantile-Quantile comparison of gridded QUIKSCAT data between QSCAT-1 model function and QSCAT-1/ F-13 model function. Adjustment based on correction (Fit to < 5%) applied in MSC50 hindcast and hindcast data for this study.

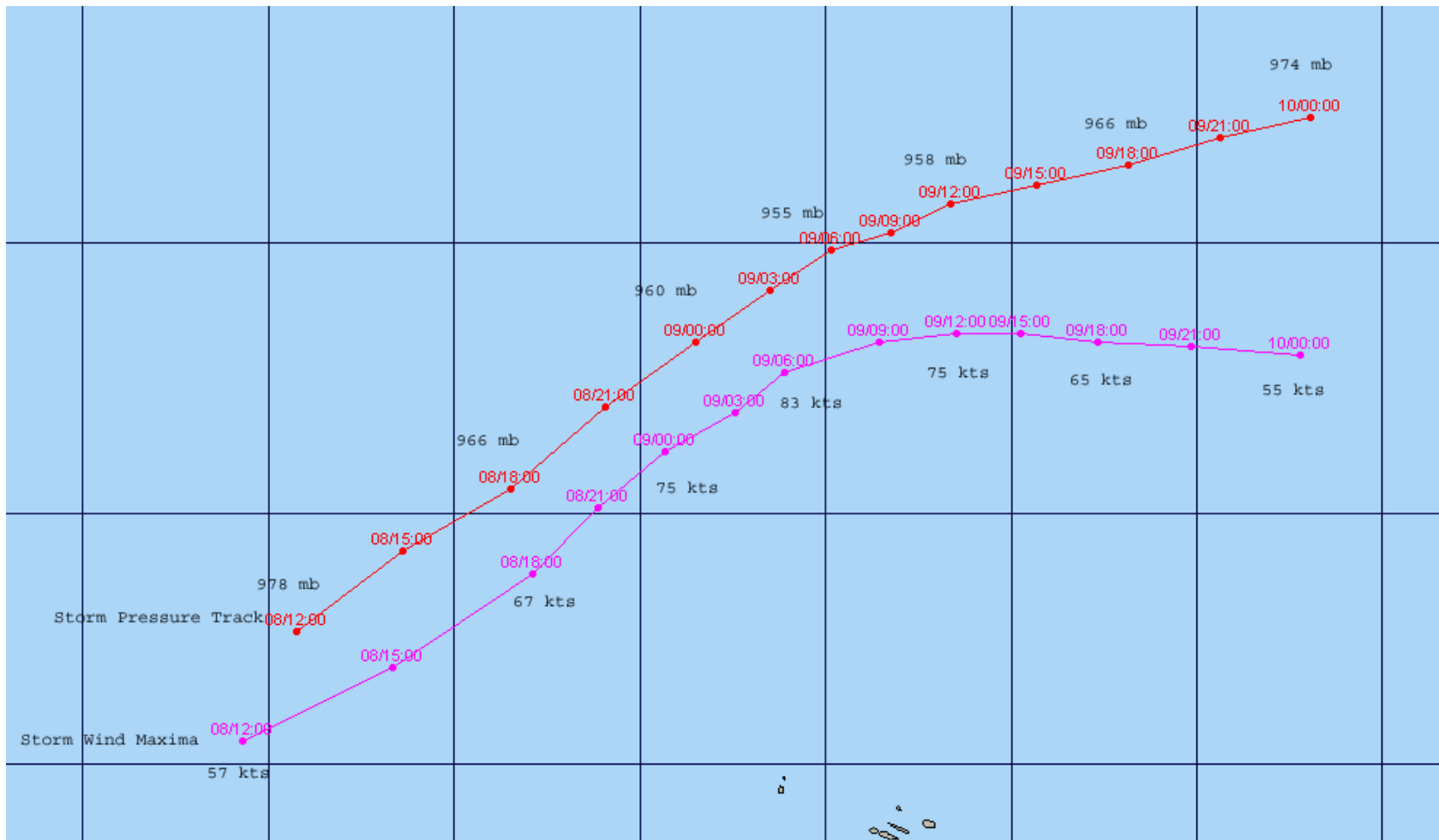


Figure 5 Adopted storm pressure track (red) and wind field maxima (purple) during the storm period of Feb-8 12 UTC to Feb-10 00 UTC 2007

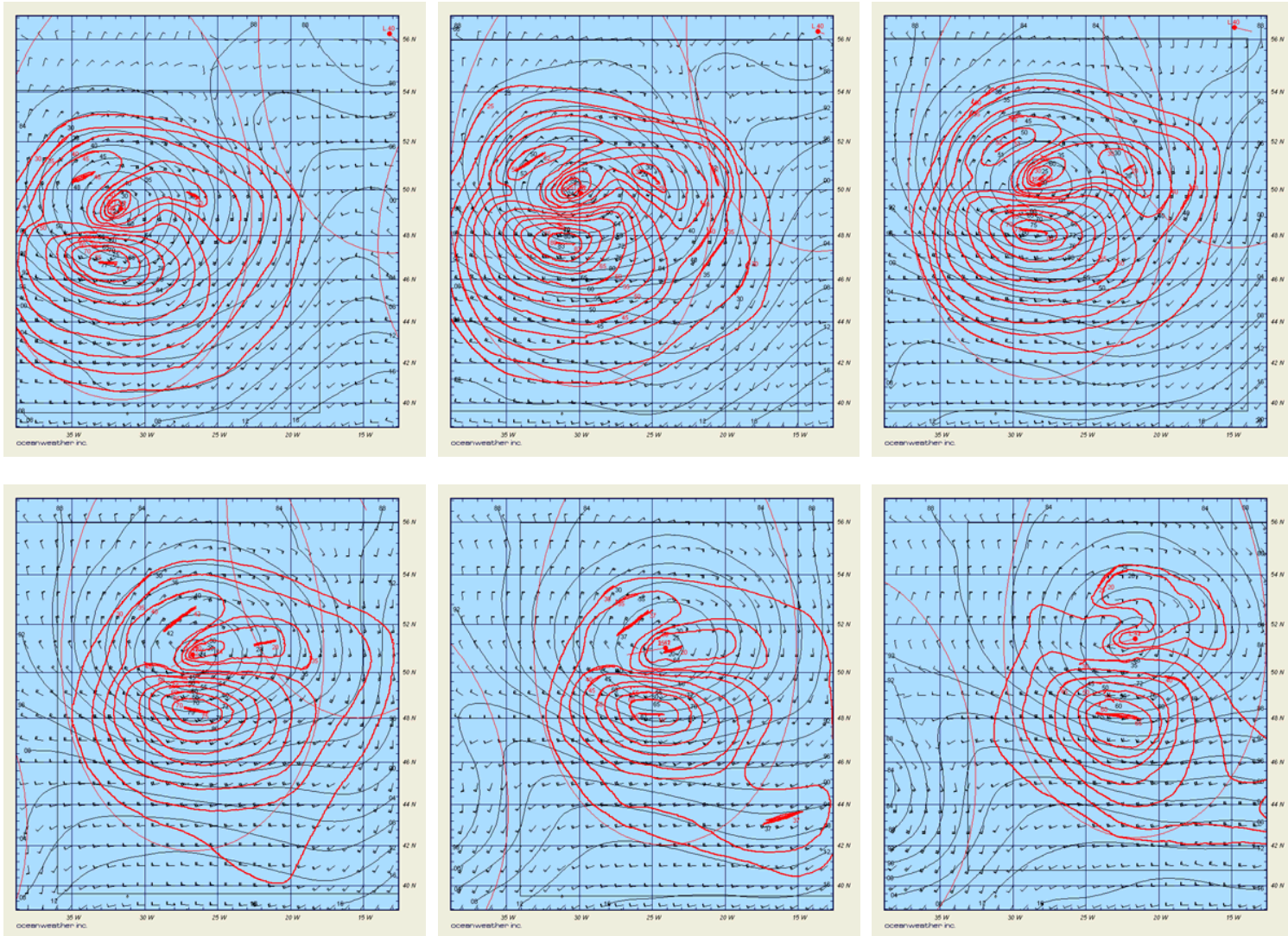


Figure 6. Six-hourly sequence of wind speed isotach analysis (knots, red) with sea level pressures (mb, black) from Feb-8 12 UTC to Feb-10 00 UTC 2007.

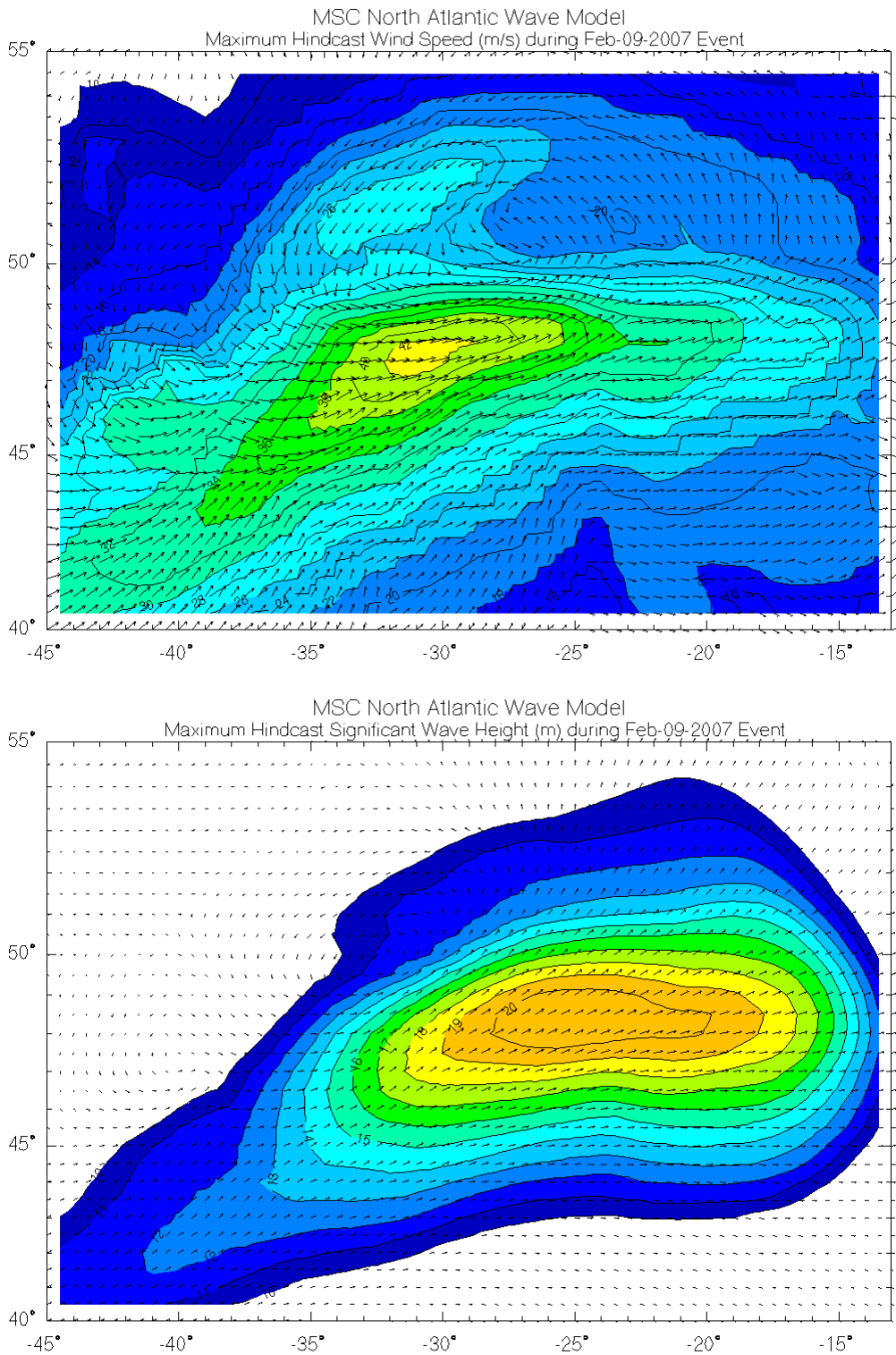


Figure 7 Maximum hindcast wind speed (m/s, top) and significant wave height (m, bottom) during Feb 2007 storm

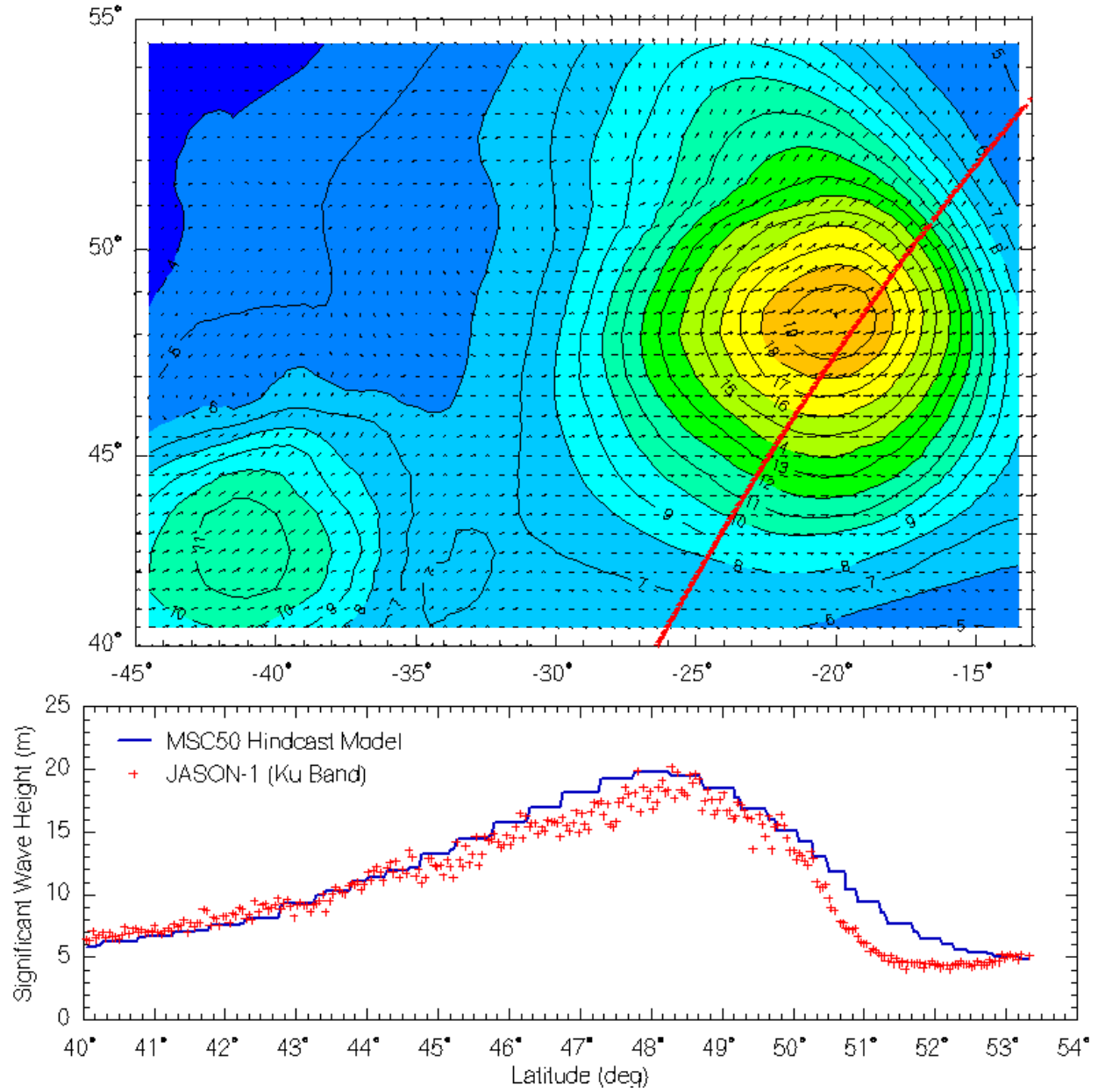


Figure 8 Comparison of hindcast and JASON altimeter transect at Feb-07-2007 21 UTC

REFERENCES

- Bancroft, G. P., 2007: Marine Weather Review – North Atlantic Area January through April, 2007. *Mariners Weather Log*, 51, 38-53.
- Buchner, B. and T. Bunnik 2007. Extreme Wave Effects on Deepwater Floating Structures. Offshore Technology Conference paper 18493, April 2007.
- Cardone, V. J., R. E. Jensen, D. T. Resio, V. R. Swail and A. T. Cox, 1996. Evaluation of contemporary ocean wave models in rare extreme events: Halloween storm of October, 1991; Storm of the century of March, 1993. *J. of Atmos. And Ocean. Tech.*, 13, 198-230.
- Cardone V.J., A.T. Cox, E.L. Harris, E.A. Orelup, M.J. Parsons and H.C. Graber. Impact of QuikSCAT Surface Marine Winds on Wave Hindcasting. 8th International Wind and Wave Workshop, Oahu, Hawaii November 14-19, 2004.
- Cox, A. T., J. A. Greenwood, V. J. Cardone, and V. R. Swail, 1995: An interactive objective kinematic analysis system. Proceedings of the 4th International Workshop on Wave Hindcasting and Forecasting, October 16-20, 1995. Banff, Alberta, Canada, p. 109-118.
- Cox, A.T., V. Cardone, F. Counillon, and C. Szabo, 2005. Hindcast Study of Winds, Waves and Currents in Northern Gulf of Mexico in Hurricane Ivan, OTC 17736, Houston Texas, Offshore Technology Conference, May 2005.
- Cardone, V.J., A.T. Cox and G.Z. Forristall, 2007: OTC 18652: Hindcast of Winds, Waves and Currents in Northern Gulf of Mexico in Hurricanes Katrina (2005) and Rita (2005). 2007 Offshore Technology Conference, May 2007, Houston, TX.
- Durrant, Tom H. , Diana J. M. Greenslade, Ian Simmonds (2009) Validation of Jason-1 and Envisat Remotely Sensed Wave Heights, 123. In *Journal of Atmospheric and Oceanic Technology* 26 (1).
- Forristall, G.Z. and J. A. Greenwood, 1998. Directional spreading of measured and hindcasted wave spectra. Proc. 5th International Workshop on Wave Hindcasting and Forecasting, Melbourne, FL, January 26-30, 1998
- Forristall, G.Z. 2006. Comparing Hindcasts from Wave Measurements from Hurricanes Lili, Ivan, Katrina and Rita. American Petroleum Institute report.
- Garrett, C. and J. Gremuch 2009. Rogue Waves. *Physics Today*, American Institute of Physics, June 2009
- Holliday, N. P., M. J. Yelland, R. Pascal, V. R. Swail, P. K. Taylor, C. R. Griffiths, and E. Kent (2006), Were extreme waves in the Rockall Trough the largest ever recorded?, *Geophys. Res. Lett.*, 33, L05613, doi:10.1029/2005GL025238.
- Janssen, B. Hansen, and J. R. Bidlot, 1997: Verification of the ECMWF wave forecasting system against buoy and altimeter data. *Wea. Forecasting*, 12, 763–784.

Jensen, R.E., V.J. Cardone and A.T. Cox, 2006: Performance of Third Generation Wave Models in Extreme Hurricanes. 9th International Wind and Wave Workshop, September 25-29, 2006, Victoria, B.C.

Khandekar, M. L., R. Lalbeharry and V. J. Cardone. 1994. The performance of the Canadian spectral ocean wave model (CSOWM) during the Grand Banks ERS-1 SAR wave spectra validation experiment. Atmosphere-Oceans, 32, 31-60.

Magnusson, A.K., M. Reistad, O. Breivik, R. Myklebust and E. Ash 2006. Forecasting a 100-Year Wave Event. 9th International Workshop on Wave Hindcasting, Victoria, B.C. Sept. 24-29, 2006.

Picot, N., K. Case, S. Desai and P. Vincent 2003. AVISO and PODAAC User Handbook. IGDR and GDR Jason Products. SMM-MUM5-OP-13184-CN (AVISO), JPL D-21352 (PODAAC).

Powell, M. D., S. Murillo, P. Dodge, E. Uhlhorn, J. Gamache, V. Cardone, A. Cox, S. Otero, N. Carrasco, B. Annane and R. St. Fleur, 2008. Reconstruction of Hurricane Katrina's Wind field for Storm Surge and Wave Hindcasting. Ocean Engineering (in print)

Queffeuilou, P. (2004). Long-Term Validation of Wave Height Measurements from Altimeters. Marine Geodesy. 27. pp. 495-510.

Queffeuilou, P. (2003). Cross-validation of ENVIRSAT RA-2 significant wave height, σ_0 , and wind speed. IFREMER Final report, May 2003.

QuikSCAT Science Data Product User's Manual. Overview & Geophysical Data Products. Version 3.0. Sept. 2006, D-1805-Rev A.

Sanders, F. and J. R. Gyakum, 1980: Synoptic-dynamic climatology of the "Bomb". Mon. Wea. Rev, 108, 1589-1606.

Soares and Swail, 2006. The WMO/IOC JCOMM Wave Programme. 9th International Wind and Wave Workshop, Victoria, B.C. Sept. 25-29, 2006.

Swail, V.R., V.J. Cardone, M. Ferguson, D.J. Gummer, E.L. Harris, E.A. Orelup and A.T. Cox, 2006 The MSC50 Wind and Wave Reanalysis. 9th International Wind and Wave Workshop, September 25-29, 2006, Victoria, B.C.

Von Ahn, J.M., Sienkiewicz and P. Chang, 2006: Operational impact of QuikSCAT winds in the NOAA Ocean Prediction Center. Weather and Forecasting, 21,523-539.